Chemical Science

Accepted Manuscript

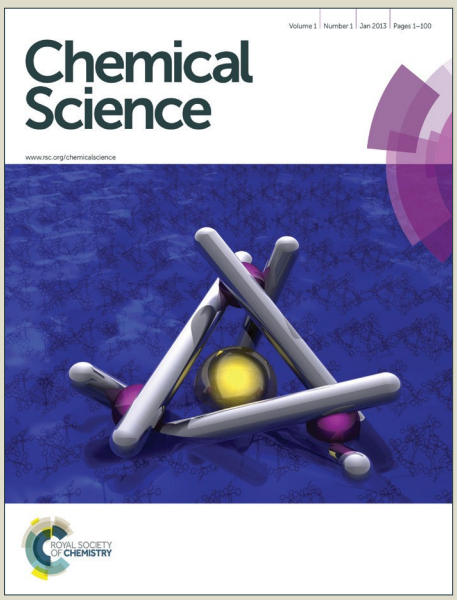

ROYAL SOCIETY OF CHEMISTRY

www.rsc.org/chemicalscience

Cite this: DOI: 10.1039/c0xx00000x

www.rsc.org/xxxxxx

ARTICLE TYPE

Protein-specific Raman imaging of glycosylation on single cells with zone-controllable SERS effect†

Yunlong Chen,‡[a] Lin Ding,‡[a] Wanyao Song,[a] Min Yang,[b] and Huangxian Ju*[a]

Received (in XXX, XXX) Xth XXXXXXXXX 20XX, Accepted Xth XXXXXXXXX 20XX

DOI: 10.1039/b000000x

A zone-controllable SERS effect is presented for Raman imaging of protein-specific glycosylation on cell surface using two types of newly designed nanoprobes. The signal probe, prepared using a Raman signal molecule and dibenzocyclooctyne-amine to functionalize 10-nm Au nanoparticle, exhibits negligible SERS effect and can recognize and link the azide-tagged glycan via a click reaction. The substrate probe, an aptamer modified 30 or 40-nm Au nanoparticle, can specifically recognize the target protein to create efficient SERS zone on target protein. By controlling the size of the substrate probe to match the expression zone of protein-specific glycan, the efficient SERS signal can be generated. This method has been successfully used for in situ imaging of sialic acids on the target protein EpCAM on MCF-7 cell surface and monitoring of the expression variation of protein-specific glycosylation during drug treatment. The concept of zone control can also be used to measure the space distance of glycoproteins on cell surface. This protocol shows its prospect in uncovering glycosylation-related biological processes.

Introduction

Glycosylation is one of the most common post-transcriptional modifications of proteins in eukaryotes. Aberrant protein glycosylation profoundly affect cellular adhesion or motility, which further reflects the physiological and pathological states of cells.[1-3] Thus in situ visualization of glycans on specific protein may provide the correlation of protein glycosylation with disease state for uncovering their roles in disease development. Several Förster resonance energy transfer (FRET) methods have been developed for imaging of protein-specific glycans by labeling protein and the corresponding glycan with two FRET-achievable fluorescent molecules.[4-6] However, one donor-to-one acceptor FRET mode cannot provide the integral glycan signal on target protein that is generally modified with more than one glycan. Besides, the short FRET distance between donor and acceptor[7] might limit its application in the study of biggish proteins. Thus development of new imaging strategies for monitoring the glycosylation of specific protein is still an urgent demand.

Raman imaging based on surface-enhanced Raman scattering (SERS) is a promising non-destructive and photo bleaching-less biological imaging technique.[8-10] It possesses high imaging sensitivity.[11-14] Different from the FRET, all Raman reporter molecules in substrate vicinity can be enhanced.[15-17] To provide the exact glycosylation information of target protein, here we design a zone-controllable SERS effect by controlling the size of substrate to match the expression zone of protein-specific glycan (Fig. 1), which leads to a strong SERS signal for Raman imaging of protein-specific glycans on cell surface. Moreover, the concept of zone control can also be used for in situ measurement of the space distance of glycoproteins on cell surface.

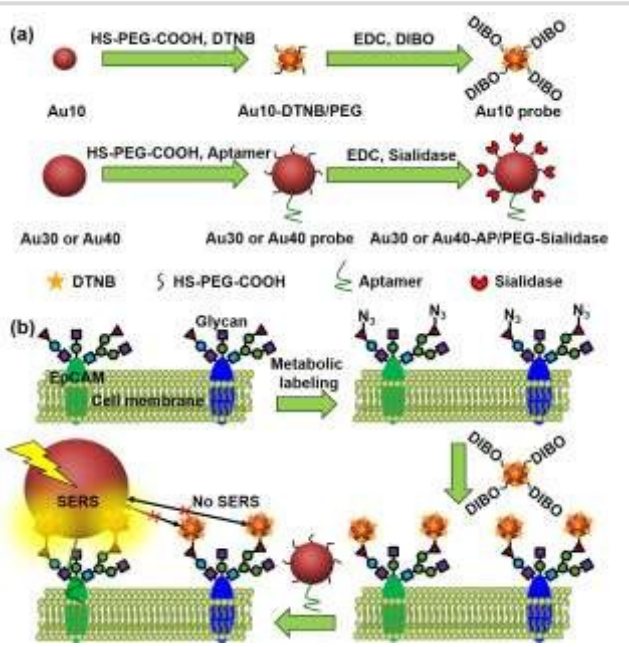

Fig. 1 Schematic illustration of (a) synthesis of two types of Au nanoprobes and (b) Zone-controllable SERS effect for imaging of protein-specific glycans on cell surface.

[a] *State Key Laboratory of Analytical Chemistry for Life Science, School of Chemistry and Chemical Engineering, Nanjing University, Nanjing 210023, P.R. China. Fax/Tel.: +86 25 89683593; E-mail: hxju@nju.edu.cn*

[b] *Department of Pharmaceutical & Biological Chemistry, UCL School of Pharmacy, University College London, London WC1N 1AX, UK*

† Electronic Supplementary Information (ESI) available: Experimental details and supplementary figures. See DOI: 10.1039/b000000x/

‡ Y. L. Chen and L. Ding contributed equally to this work.

Generally the optimum size of nano-substrates for SERS is 30-100 nm.[18] To achieve the zone-controllable SERS effect, the Au nanoparticles (AuNP) with diameter of 10 nm (Au10), having negligible SERS effect, were chosen to load Raman signal molecule, 5,5′-dithiobis (2-nitrobenzoic acid) (DTNB), and 30-nm, the lowest limit for producing the SERS effect,[18] or 40-nm AuNPs (Au30 or Au40) were used as SERS substrate to select the efficient zone of SERS effect. The glycan recognition ability of DTNB-loaded Au10 was acquired with a cyclooctyne terminal (DIBO) through a polyethylene glycol (PEG) linker, which could link azide group through copper-free click chemistry.[19,20] The azide group was formed on the terminal site of glycan chains with a metabolic glycan labeling technique.[21-23] The cell surface protein recognition was achieved by modifying the Au30 or Au40 with aptamer (substrate probe, Au30 or Au40 probe). Here the liberally foldable structure of the aptamer was important for guiding the probe to the site of target protein.[24-26] Upon the stepwise recognition of Au10 probe to target glycan on target protein and substrate probe to the protein on cell surface, two probes approached enough to produce SERS effect and the Raman signal of DTNB, which could be used for in situ protein-specific Raman imaging of glycosylation on cell surface. The designed strategy successfully achieved the in situ detection of sialic acids of target protein EpCAM on MCF-7 cell surface and the monitoring of the expression variation of protein-specific glycosylation during drug treatment. This work provided a powerful protocol for uncovering glycosylation-related biological processes at protein-specific level.

Results and discussion

Characterization of AuNP probes

The AuNPs with different sizes were firstly characterized with TEM and dynamic light scattering (Fig. S1†), which showed a narrow size distribution. The Au10 probe showed the characteristic infrared absorption peak of alkyne group in DIBO around 2160 cm^{-1} (Fig. 2a) and the Raman spectrum similar to that of DTNB (Fig. 2b), which demonstrated the presence of DIBO and DTNB and indicated the successful synthesis of Au10 probe. The UV spectra of the substrate probes showed the characteristic absorption peak of DNA at 260 nm (Fig. 2c and inset in Fig. 2c), indicating the binding of aptamer to Au30 and Au40. The Au30- and Au40-AP/PEG-sialidase showed wider absorbance around 250-290 nm due to the overlap of protein absorbance (Fig. 2c and inset in Figure 2c), which confirmed the binding of sialidase to these probes. Considering that PEG, aptamer and sialidase are negatively charged, the zeta potentials with step-by-step change upon each synthesis step of two types of probes further confirmed their successful modification (Fig. 2d-f). The amounts of aptamer bound on each Au40 and Au30 probe were estimated to be 220 and 150 by UV measurement of the collected supernatant containing excess aptamer during probe preparation, respectively (Fig. S2†).

Verification of dual-probe system

To verify the feasibility of the proposed dual-probe nanostructure for generating the SERS effect, PDDA-Au40 charged positively

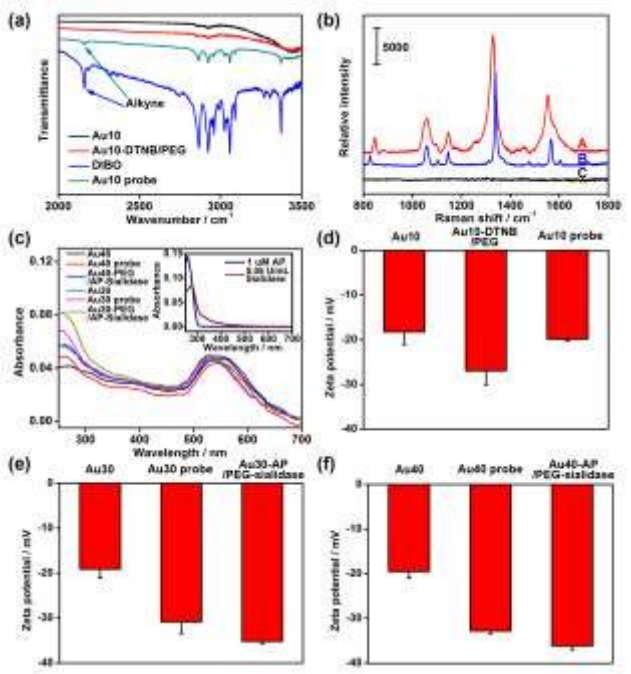

Fig. 2 (a) Infrared spectra of Au10, Au10-DTNB/PEG, DIBO and Au10 probe. (b) Raman spectra of the solid powder of Au10 probe (A), DTNB (B) and Au10-PEG-DIBO (C). (c) UV spectra of 1 nM Au40, Au40 probe, Au40-AP/PEG-sialidase, Au30, Au30 probe and Au30-AP/PEG-sialidase. Inset: UV spectra of 1 μM aptamer and 0.05 U/mL sialidase. Zeta potentials of (d) Au10, Au10-DTNB/PEG, Au10 probe, (e) Au30, Au30 probe, Au30-AP/PEG-sialidase and (f) Au40, Au40 probe, Au40-AP/PEG-sialidase.

(Fig. 3a) was prepared to simulate the approach of Au10 probe and substrate probe to generate the SERS effect. The Raman spectra of both Au10 probe and the mixture of Au40 probe and Au10 probe did not show the characteristic peaks of DTNB (Fig. 3b, B and C), suggesting the absence of the SERS effect in their free states and the tiny Raman background for Raman imaging. After replacing the Au40 probe with PDDA-Au40, which did not exhibit any Raman response (Fig. 3b, A), the mixture showed strong characteristic peaks of DTNB due to the electrostatic adsorption of Au10 probe on PDDA-Au40 (Fig. 3b, F). This result indicated the adsorption brought the DTNB and Au40 close to generate SERS and the designed dual-probe nanostructure can successfully generate SERS when the two-hetero-Au probes are in proximity. The peak intensities were about two times stronger

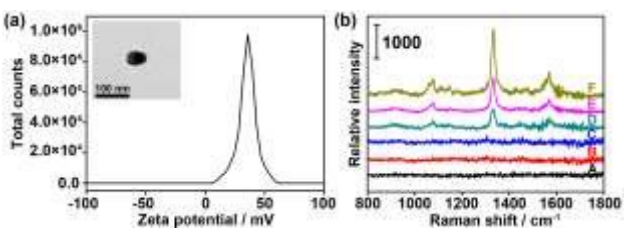

Fig. 3 (a) Zeta potential of PDDA-Au40. Inset: TEM image of PDDA-Au40. (b) Raman spectra of (A) 1 nM PDDA-Au40 and (B) 10 nM Au10 probe in PBS, (C) mixture of 10 nM Au10 probe and 1 nM Au40 probe in PBS, (D) 1 nM PDDA-Au40 after incubation with 100 μM DTNB, (E) 10 nM Au10 added in (D), (F) 1 nM PDDA-Au40 after incubation with 10 nM Au10 probe.

than that of DTNB-adsorbed PDDA-Au40 after further loaded with bare Au10 (Fig. 3b, E), and four times stronger than that of DTNB-adsorbed PDDA-Au40 without presence of Au10 (Fig. 3b, D), indicating greater loading capacity of Raman reporter on Au10 probe, and higher SERS efficiency of the dual-AuNP nanostructure formed in the dual recognition process. The dual-AuNP nanostructure could generate stronger plasmonic field enhancements.[27-29] Thus the dual-probe nanostructure can produce highly sensitive signal for double recognition triggered high-quality Raman imaging.

Labeling capability

Prior to Raman imaging of protein-specific glycans on cell surface, the labeling capability of the recognition pairs was examined. Epithelial cell adhesion molecule (EpCAM) on human breast cancer MCF-7 cells[30] was used as the target protein, which is composed of 314 amino acids and contains three N-linked glycosylation sites but no O-linked glycosylation site,[31] and tetraacetylated N-azidoacetyl-D-mannosamine (ManNAz) was used to metabolically label cell surface sialic acid (Sia) as target glycan.[32,33] Tetraacetylated N-azidoacetylgalactosamine (GalNAz) and tetraacetylated N-azidoacetylglucosamine (GlcNAz), which can metabolically label cell surface O-linked glycans (OLG)[32,33] and intracellular O-linked N-acetylglucosamine,[33,34] respectively, were used as negative controls. The existence of EpCAM on MCF-7 cells was firstly confirmed with flow cytometric analysis. The MCF-7 cells exhibited strong binding to both EpCAM antibody and aptamer, while Ramos cells as the control did not exhibit fluorescence signal (Fig. S3†). Confocal fluorescence imaging of metabolic-labeled MCF-7 cells was performed with dual-color labeling of EpCAM and azide-labeled glycans using FITC-conjugated aptamer and Alexa Fluor 647 DIBO alkyne, respectively (Fig. 4). The images showed overlaid fluorescence signals from FITC and Alexa Fluor 647 bound at cell surface, demonstrating the efficient recognition. However, due to the strong monochrome background the fluorescence intensity was weak, and the overlay of both signals could not provide the linkage information of glycans with the protein. The specificity of aptamer-EpCAM recognition was further verified using a FITC-labeled random DNA sequence (RS), which did not exhibit the signal of FITC (Fig. 4). The recognition-mediated adjacent localization of two Au probes on metabolically labeled cell surface could be observed by TEM images (Fig. S4†). Although the possible crosslinking of several molecules to each probe might happen, it did not affect the monitoring of glycosylation level change of specific protein.

Zone-controllable SERS imaging

To obtaining high-quality Raman images, the incubation times of three metabolic reagents were optimized to be 48 h using confocal fluorescence imaging with Alexa Fluor 647 DIBO alkyne (Fig. S5†), and the incubation times of two Au probes were optimized to be 30 min by confocal Raman imaging (Fig. S6†). In such a short time the altering of the glycoprotein properties could be neglected.

Under the optimal incubation conditions, three types of glycans on cell surface EpCAM were imaged with the zone-controllable SERS strategy using both Au40 and Au30 probes, respectively. The specificity of SERS imaging is mainly decided by the

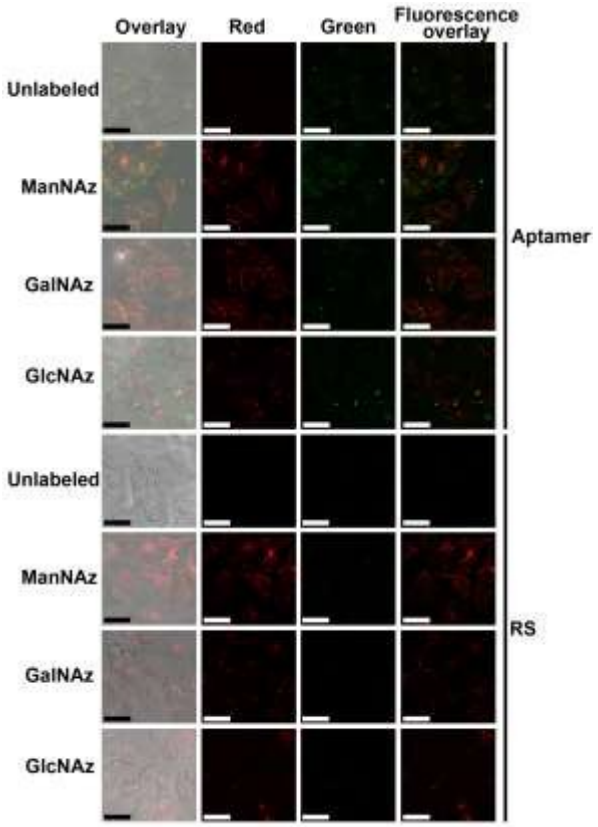

Fig. 4 Confocal fluorescence images of unlabeled, and ManNAz, GalNAz and GlcNAz metabolically labeled cells after incubation with 25 μM Alexa Fluor 647 DIBO alkyne for 30 min and then 1 μM FITC-labeled aptamer or random sequence for 30 min. From left to right: overlay, Alexa Fluor 647 fluorescence (red), FITC fluorescence (green) and dual fluorescence overlay images. Scalar bar: 30 μm.

efficient SERS zone of the substrate probe. Chlorpromazine was used as an endocytosis inhibitor during the interaction between probe and cells. When Au40 probe was used, the ManNAz andGalNAz labeled cells showed obvious Raman signal on cell surface, which were negligible on unlabeled cells or in GlcNAz labeled cells (Fig. 5). In the case of Au30 probe, only ManNAz

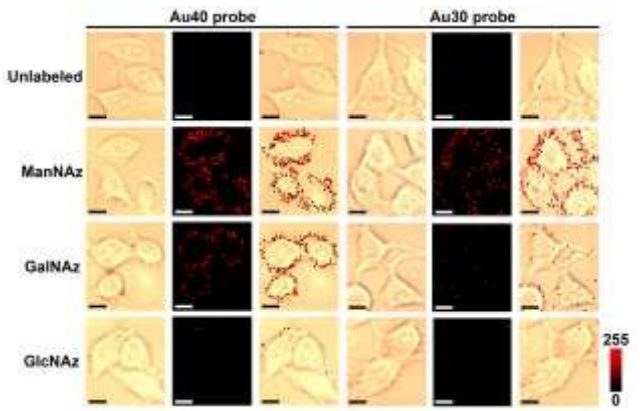

Fig. 5 Bright field, Raman and overlay images of unlabeled, and ManNAz, GalNAz and GlcNAz metabolically labeled MCF-7 cells after treated with different substrate probes. Scalar bar: 10 μm.

labeled cells showed obvious Raman signal. The negligible signal on unlabeled cell surface indicated the binding of Au10 probe with metabolically labeled cells was specific. Both the negligible signal in GlcNAz labeled cells and the membrane-distributed signal excluded the endocytosis of the substrate probes, which was attributed to the high hydrophilicity of PEG on probe as well as the short treatment time. Considering the absence of O-linked glycosylation site on EpCAM,[31] the signal of GalNAz labeled cells treated with Au10 and Au40 probes could be attributed to the OLG on the neighbouring glycoproteins, thus the absence of GalNAz signal indicated that the efficient SERS zone of Au30 probe was appropriate for the zone of glycans expressed on EpCAM, while Au40 probe was too large. The protein-specific glycan expression zone could be more accurately matched with more kinds of substrate probe to precisely control the size. But the smallest radius of 15 nm of nano-substrates for efficient SERS effect[18] limits the detection precision of this method for smallish proteins. FRET based protein-specific imaging[4-6] is a more appropriate detection technique for the protein with smallish glycan expression zone.

Since Au40 probe might interact with Au10 probe from neighboring non-EpCAM glycoproteins while Au30 probe did not, the general distance between EpCAM and its neighboring glycoproteins could be estimated to be about 20-25 nm if the minimum requirement for SERS was not considered. Thus the proposed zone-controllable strategy might be potentially used to in situ measure the space distance of glycoproteins on cell surface. Although one report suggested the possible interconversion between GlcNAz and GalNAz by epimerase,[35] the negligible signal for GlcNAz labelling indicated the conversion rate was very limited. The signal of Raman imaging kept stable at 24, 48 and 72 hours after the first imaging, which confirmed the stability of the Raman imaging strategy (Fig. S7†).

Compared with the fluorescence images with dual-color labeling (Fig. 4), the Raman images could not only give the glycan information on specific protein but also exhibit higher intensity and tiny background noise. The EpCAM-negative Ramos cells showed very weak Raman signal for all the three types of metabolic labeling (Fig. S8†). This further confirmed that only EpCAM-specific glycan could be imaged with the proposed method. The specificity of aptamer-functionalized probe toward EpCAM was also verified using a RS and PEG co-modified Au40 (Au40-RS/PEG) to replace Au40 probe, which could not generate obvious Raman signal (Fig. S8†). This result was consistent with that of fluorescence imaging (Fig. 4). After EpCAM knockdown with RNAi experiment,[30] both Raman and fluorescence signals disappeared (Fig. S9†), which further verified the specificity of protein recognition.

Monitoring of glycan cleavage and protein-specific glycosylation variation

Since Au30 probe is more size-appropriate for EpCAM-Sia imaging, the proposed strategy could be used to cleave protein-specific glycan by treating with cleaving nanoparticles, Au30-AP/PEG-sialidase (Fig. 1). After the specific recognition of Au10 probe to cell surface Sia, and the aptamer-mediated binding of Au30-AP/PEG-sialidase to cell surface EpCAM, the cells were

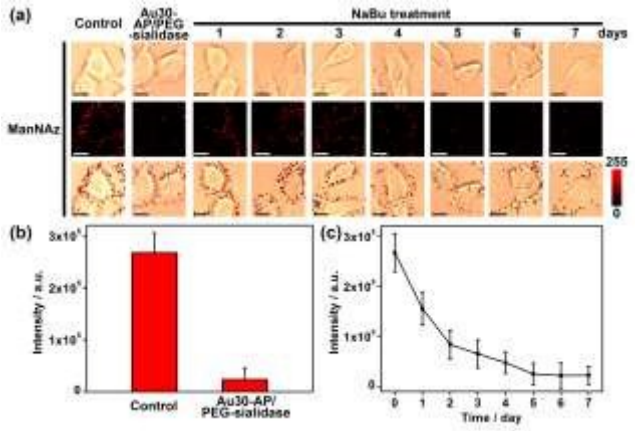

Fig. 6 (a) Bright field, Raman and overlay images of ManNAz metabolically labeled MCF-7 cells as control and these cells treated with Au30-AP/PEG-sialidase or NaBu. Scalar bar: 10 μm. (b) Raman intensity obtained from a). (c) Plots of Raman intensity *vs.* NaBu incubation time.

incubated in PBS (pH 7.4) for 30 min, during which the bound sialidase could cleave the Sia under the coverage area of Au30 probe. The confocal Raman images of these cells showed obviously decreased signal for Sia on EpCAM (Fig. 6a and 6b). This result shows the proposed zone-controllable effect could be used as a powerful glycan cleavage tool at protein-specific level.

To verify the practicability of the proposed method, MCF-7 cells were firstly treated with 1 mM sodium butyrate (NaBu) for different times, then labeled with ManNAz and recognized by Au10 and Au30 probes. With the increasing treatment time from 1 to 7 days, the Raman images of these labeled cells showed obviously decreased signal (Fig. 6a and 6c). These results indicated the decrease of EpCAM-specific Sia expression on MCF-7 cell surface, which could be attributed to the down-regulation of EpCAM expression during NaBu treatment[36] (Fig.

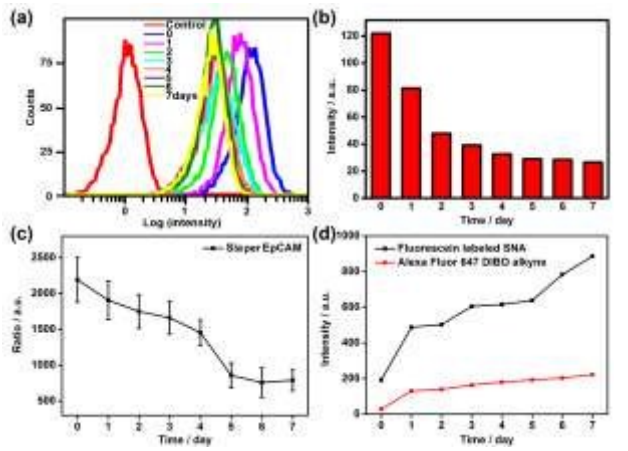

Fig. 7 (a) Flow cytometric detection and (b) mean fluorescence intensity of MCF-7 cells treated with 1 mM NaBu for 0-7 days and subsequently incubated with FITC-conjugated EpCAM anti. (c) Plot of ratio of average Raman intensity of ManNAz metabolically labeled MCF-7 cells after two-probe incubation to corresponding average EpCAM fluorescence intensity *vs.* NaBu treatment time. (d) Plot of mean flow cytometric fluorescence intensity of ManNAz metabolically labeled MCF-7 cells after incubation with fluorescein labeled SNA or Alexa Fluor 647 DIBO alkyne *vs.* NaBu treatment time.

7a and 7b). By dividing the average Raman intensity corresponding to EpCAM-specific Sia during the NaBu treatment period with the average fluorescence intensity of EpCAM in flow cytometric analysis, the variation trend of Sia expression on each EpCAM protein could be estimated (Fig. 7c). The Sia expression level on each EpCAM showed a certain degree of decrease with the increasing NaBu treatment time. On the contrary, with regard to whole cell surface glycan expression detected with the corresponding lectin or Alexa Fluor 647 DIBO alkyne, the NaBu treatment led to the increased Sia expression (Fig. 7d). The increasing expression of Sia on the whole cell surface under NaBu treatment might be due to the up-regulated glycosylation of other glycoproteins.[37,38] These results indicated that the proposed methods could reflect the glycosylation level change of specific protein to a certain degree. Thus the strategy based on zone-controllable SERS effect possessed great importance and effective applicability for in situ monitoring protein-specific glycosylation on cell surface.

Conclusions

In conclusion, the designed zone-controllable SERS effect has been successfully used for protein-specific Raman imaging of glycosylation by matching the size of the substrate probe with the expression zone of protein-specific glycan. This effect can be used for in situ monitoring the cleavage of protein-specific glycan and obtaining the glycosylation variation information of each specific protein. Besides, the conception of zone control could be used for in situ measuring the space distance of glycoproteins on cell surface. Since Raman imaging can provide detailed spectrum information, the proposed method leads to the potential for multi-component research. By combining with other biological labeling technologies, this strategy shows a broad applicability for other proteins which provides a promising protocol for investigation of glycosylation-related biological processes at protein-specific level.

Acknowledgements

This work was financially supported by National Natural Science Foundation of China (91213301, 91413118, 21135002, 21322506) and National Basic Research Program (2014CB744501). Y.C. thanks the Scientific Research Foundation of Graduate School of Nanjing University (2013CL01) and Graduate Innovation Project of Jiangsu Province (KYZZ-0028).

Notes and references

1 K. Ohtsubo, S. Takamatsu, M. T. Minowa, A. Yoshida, M. Takeuchi, and J. D. Marth, *Cell* 2005, **123**, 1307–1321.
2 S. K. Cha, B. Ortega, H. Kurosu, K. P. Rosenblatt, M. Kuroo, and C. L. Huang, *Proc. Natl. Acad. Sci. U.S.A.* 2008, **105**, 9805–9810.
3 M. M. Fuster, and J. D. Esko, *Nat. Rev. Cancer* 2005, **5**, 526–542.
4 Y. Haga, K. Ishii, K. Hibino, Y. Sako, Y. Ito, N. Taniguchi, and T. Suzuki, *Nat. Commun.* 2012, **3**, 907.
5 B. Belardi, A. de la Zerda, D. R. Spiciarich, S. L. Maund, D. M. Peehl, and C. R. Bertozzi, *Angew. Chem. Int. Ed.* 2013, **52**, 14045–14049.
6 W. Lin, Y. F. Du, Y. T. Zhu, and X. Chen, *J. Am. Chem. Soc.* 2014, **136**, 679–687.
7 J. Zheng, *Methods Mol. Biol.* 2006, **337**, 65–77.
8 S. Keren, C. Zavaleta, Z. Cheng, A. de la Zerda, O. Gheysens, and S. S. Gambhir, *Proc. Natl. Acad. Sci. U.S.A.* 2008, **105**, 5844–5849.
9 X. M. Qian, X. H. Peng, D. O. Ansari, Q. Yin-Goen, G. Z. Chen, D. M. Shin, L. Yang, A. N. Young, M. D. Wang, and S. M. Nie, *Nat. Biotechnol.* 2008, **26**, 83–90.
10 Z. Liu, X. L. Li, S. M. Tabakman, K. L. Jiang, S. S. Fan, and H. J. Dai, *J. Am. Chem. Soc.* 2008, **130**, 13540–13541.
11 Y. Q. Wang, B. Yan, and L. X. Chen, *Chem. Rev.* 2013, **113**, 1391–1428.
12 H. Abramczyk and B. Brozek-Pluska, *Chem. Rev.* 2013, **113**, 5766–5781.
13 W. T. Lu, A. K. Singh, S. A. Khan, D. Senapati, H. T. Yu, and P. C. Ray, *J. Am. Chem. Soc.* 2010, **132**, 18103–18114.
14 L. Guerrini, E. Pazos, C. Penas, M. E. Vázquez, J. L. Mascareñas, and R. A. Alvarez-Puebla, *J. Am. Chem. Soc.* 2013, **135**, 10314–10317.
15 J. R. Lombardi, and R. L. Birke, *Acc. Chem. Res.* 2009, **42**, 734–742.
16 W. Xie, P. H. Qiu, and C. B. Mao, *J. Mater. Chem.* 2011, **21**, 5190–5202.
17 T. Ichimura, S. Fujii, P. Verma, T. Yano, Y. Inouye, and S. Kawata, *Phys. Rev. Lett.* 2009, **102**, 186101.
18 M. Moskovits, *J. Raman Spectrosc.* 2005, **36**, 485–496.
19 J. C. Jewett, E. M. Sletten, and C. R. Bertozzi, *J. Am. Chem. Soc.* 2010, **132**, 3688–3690.
20 X. H. Ning, J. Guo, M. A. Wolfert, and G. J. Boons, *Angew. Chem. Int. Ed.* 2008, **47**, 2253–2255.
21 S. T. Laughlin and C. R. Bertozzi, *Proc. Natl. Acad. Sci. U.S.A.* 2009, **106**, 12–17.
22 R. Xie, S. L. Hong, and X. Chen, *Curr. Opin. Chem. Biol.* 2013, **17**, 747–752.
23 R. Xie, S. L. Hong, L. S. Feng, J. Rong, and X. Chen, *J. Am. Chem. Soc.* 2012, **134**, 9914–9917.
24 X. Fang and W. Tan, *Acc. Chem. Res.* 2010, **43**, 48–57.
25 R. R. Breaker, *Nature* 2004, **432**, 838–845.
26 J. Mi, Y. Liu, Z. N. Rabbani, Z. Yang, J. H. Urban, B. A. Sullenger, and B. M. Clary, *Nat. Chem. Biol.* 2010, **6**, 22–24.
27 N. J. Halas, S. Lal, W. S. Chang, S. Link , and P. Nordlander, *Chem. Rev.* 2011, **111**, 3913–3961.
28 J. P. Camden, J. A. Dieringer, J. Zhao, and R. P. Van Duyne, *Acc. Chem. Res.* 2008, **41**, 1653–1661.
29. E. C. Le Ru and P. G. Etchegoin, *Chem. Phys. Lett.* 2004, **396**, 393–397.
30 W. A. Osta, Y. Chen, K. Mikhitarian, M. Mitas, M. Salem, Y. A. Hannun, D. J. Cole, and W. E. Gillanders, *Cancer Res.* 2004, **64**, 5818–5824.
31 J. M. Chong and D. W. Speicher, *J. Biol. Chem.* 2001, **276**, 5804–5813.
32 J. A. Prescher and C. R. Bertozzi, *Cell* 2006, **126**, 851–854.
33 S. T. Laughlin and C. R. Bertozzi, *Nat. Protoc.* 2007, **2**, 2930–2944.
34 D. J. Vocadlo, H. C. Hang, E. J. Kim, J. A. Hanover, and C. R. Bertozzi, *Proc. Natl. Acad. Sci. U.S.A.* 2003, **100**, 9116–9121.
35 M. Boyce, I. S. Carrico, A. S. Ganguli, S. Yu, M. J. Hangauer, S. C. Hubbard, J. J. Kohler, and C. R. Bertozzi, *Proc. Natl. Acad. Sci. U.S.A.* 2011, **108**, 3141–3146.
36 P. P. Hao, M. J. Lee, G. R. Yu, I. H. Kim, Y. G. Cho, and D. G. Kim, *Mol. Cells* 2013, **36**, 424–431.
37 H. Tateno, N. Uchiyama, A. Kuno, A. Togayachi, T. Sato, H. Narimatsu, and J. Hirabayashi, *Glycobiology* 2007, **17**, 1138–1146.
38 C. Gahmberg, M. Ekblom, and L. C. Andersson, *Proc. Natl. Acad. Sci. U.S.A.* 1984, **81**, 6752–6756.

Cite this: DOI: 10.1039/c0xx00000x

www.rsc.org/xxxxxx

ARTICLE TYPE

Table of contents

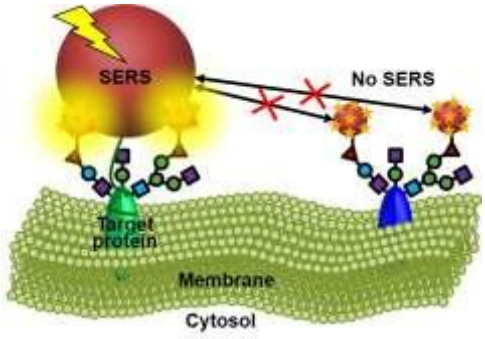

A zone-controllable SERS effect integrates controlling of nano-substrate size to match the expression zone of protein-specific glycan for Raman imaging.